

Changeover from signalling to energy-provisioning lipids during transition from colostrum to mature milk in the giant panda (*Ailuropoda melanoleuca*)

Supplementary

Tong Zhang^{*§1}, David G. Watson¹, Rong Zhang^{1,2}, Rong Hou³, I. Kati Loeffler^{3#}, and

Malcolm W. Kennedy^{4**}

¹Strathclyde Institute of Pharmacy and Biomedical Sciences, 161, Cathedral Street, Glasgow G4 0RE, Scotland, UK.

²Institute of Clinical Pharmacology, Guangzhou University of Chinese Medicine, No. 12 Jichang Road, Guangzhou 510405, P.R. China.

³Sichuan Key Laboratory of Conservation Biology for Endangered Wildlife, Chengdu Research Base of Giant Panda Breeding, 1375 Panda Road, Northern Suburb, Chengdu, Sichuan Province 610081, P.R. China

⁴Institute of Biodiversity, Animal Health and Comparative Medicine, and Institute of Molecular Cell and Systems Biology, College of Medical, Veterinary, and Life Sciences, Graham Kerr Building, University of Glasgow, Glasgow G12 8QQ, Scotland, UK.

[§] Current address Institute of Cancer Sciences, Wolfson Wohl Translational Cancer Research Centre, Garscube Estate, Switchback Road, Glasgow G61 1QH, UK.

[#] Current address: International Fund for Animal Welfare, 290 Summer St., Yarmouth Port, MA 02675, USA

*Corresponding author (lipidomics): Tong Zhang, tong.zhang@glasgow.ac.uk.

**Corresponding author (biology): Malcolm W. Kennedy, malcolm.kennedy@glasgow.ac.uk

Contents

Panel S1. Fine structural determination of lipids – details additional to main text Methods.

Table S1. Main lipids in giant panda milk.

Figure S1 – Changes in appearance of giant panda milk with time after birth.

Figure S2 – Time courses for selected polyunsaturated fatty acids in the milk of three giant pandas with time after birth.

Figure S3 – Comparison between the time-dependent lipid profiles of giant panda milk with lipid content of artificial milk replacers.

Figure S4 – Mass spectra of the main lipids identified in giant panda milk.

References for Supplementary.

Note – all the data obtained in this study are available from the corresponding authors.

Panel S1. Detailed structural determination of lipids – details additional to main text Materials & Methods

Following the procedures detailed in the main text, in order to focus on lipid analysis, the pre-processed lipid-chromatography – mass spectrometry (LC-MS) data were searched by accurate mass (± 3 ppm) against the Lipid Metabolites and Pathways Strategy (Lipid MAPS) Structure Database. For annotation of glycerolphospholipids including phosphatidylcholine (PC), phosphatidylethanolamine (PE), phosphatidylserine (PS) and phosphatidylinositol (PI), a well-defined formula prediction algorithm in MZMine 2.10 used previously [1] was also applied. The LC-MS signals were removed or ignored if their coefficient of variation values were $\geq 25\%$ in three separate quality control injections (YY-19d). Only a single LC-MS signal for each lipid was retained if the lipid was detected in both electrospray ionisation (ESI) positive and negative modes at the same retention time. Because the LC-MS experiments were performed in hydrophilic interaction liquid chromatography mode, polar lipids including PC, PE, PS, PI and sphingomyelin (SM) were well-retained on the silica column and separated according to their polar head group classes, whereas the non- or low-polarity lipids eluted quite early without sufficient retention. As reported in previous studies of LC-MS-based lipid analysis, some classes of lipids could be detected in both ESI positive and negative modes as forms of non-proton adduct ions (e.g. ammonium and formate adducts). As shown in Table S1, careful selection of the correct adduct forms in different ESI modes for accurate mass search of each lipid class can avoid confusion in putative annotation. Glycerolphospholipids with a single acyl tail showed slightly longer retention times than those with the same polar head but double acyl tails, which may be explained by their slight increase of hydrophilicity due to the presence of an exposed hydroxyl group in the glycerol backbone structure.

Further lipid structure elucidation was performed using collision-induced dissociation MSⁿ fragmentation in a data-dependent scan mode. Different lipid classes could be identified by their characteristic MS² fragmentation patterns representing the loss of the specific polar heads (Table S1). The fragment ions produced by losing a water molecule equivalent could be included with the phospholipids in ESI positive mode if the phospholipids have a free hydroxyl group in their backbone structures. MS³ fragmentation, especially in ESI negative mode, provided more details in structural information of the acyl tails. An example of this is given in Figure S3, depicting the MS² product ion of a phosphatidylserine that was further fragmented. The resulting MS³ fragment ions indicate the number of carbons of each acyl tail with the corresponding degree of unsaturation (18:0/22:6). In addition, the relative intensity of the fatty acid ions might imply the position of the acyl tail (*sn*-1 >

sn-2). Consequently, as shown in Figure S3, the acyl tail of 18:0 was assigned at *sn*-1 position and the 22:6 was at *sn*-2. More examples of MSⁿ spectra for the other lipid classes are shown in Figure S4.

The MSⁿ spectra of polar lipids obtained in this study accorded with the published data produced for Thermo Scientific mass spectrometers (LTQ ion trap or LTQ-Orbitrap) by the manufacturer. By careful analysis of MSⁿ spectra for each lipid class or subclass, it was found that the abundant polar lipids in giant panda milk possessed acyl chains comprising even numbers of carbons from 14 to 26 with the number of double bonds varying from 0 to 6. However, acyl chains with odd numbers of carbons were also found on both mono and diacyl glycerolphospholipids but were of low relative abundance in the giant panda milk samples. Compared to a single phospholipid species, a single triacylglycerol lipid species generated more fragment ions through the loss of heterogeneous fatty acid tails in the population of molecules (M-RCOO+H), indicating the presence of a more extensive range of isomers in the neutral than in the polar lipids.

Another explanation for the apparently low abundance of glycerolipids may lie in the interpretation of the low MS signal for this group of molecules. Glycerolipids provide low abundance MS signals because of their poor ESI performance such that the intensity of their MS signals did not provide quite the same clarity in changes in their relative concentrations in comparison with the polar lipids, despite being the major lipids in mammalian milks including that of giant panda.

In the data-dependent scan mode, the MSⁿ fragmentation was only triggered on those lipids with the highest intensities in the MS¹ scans. By careful interpretation of the MSⁿ spectra, their structures could be putatively constructed as shown in Figure S3. The characterisation of the lipids that did not require additional MSⁿ fragmentation was based on the elemental composition prediction and supplemented by the specific retention times corresponding to the lipid classes (see Table S1). Without considering the number of isomers, 403 species of lipid were putatively annotated in different classes and used for the statistical analysis given in the main text Section 3.2. More species were detected for PC and PS than for other polar lipids.

Table S1. Predominant lipids in giant panda milk

Main class	Subclass	Number of species detected	Retention time range (min)	Detected ion (ESI positive/negative)	Detected ion for comparative analysis	Characteristic fragmentation (ESI positive/negative)	Example of MS ⁿ analysis
Phosphatidylserine (PS)	Monoacyl-PS	25	11.8-12.5	M+H/M-H	M+H	M+H-(18+87+80)/M-H-87	PS (18:0/0:0)
	Diacyl-PS	38	10.8-11.5	M+H/M-H	M+H	M+H-185/M-H-87	PS (18:0/22:6)
Phosphatidylcholine (PC)	Monoacyl-PC	23	15.5-16.5	M+H/M+COOH-	M+H	M+H-(18+59)/(M+COOH-)-60	PC (18:1/0:0)
	Diacyl-PC	43	14.5-15.5	M+H/M+COOH-	M+H	M+H-59/(M+COOH-)-60	PC (16:0/16:0)
Phosphatidylinositol (PI)	Monoacyl-PI	2	5.5-6.5	M+NH ₄ +/M-H	M-H	M+NH4+-(18+259)/M-H-180	PI (20:4/0:0)
	Diacyl-PI	16	4.0-5.0	M+NH ₄ +/M-H	M-H	M+NH4+-(259+40)/M-H-180	PI (20:4/18:0)
Phosphatidylethanolamine (PE)	Monoacyl-PE	16	11.8-12.5	M+H/M-H	M-H	M+H-(18+123)/M-H-197=free fatty acid	PE (18:1/0:0)
	Diacyl-PE	19	10.5-11.5	M+H/M-H	M-H	M+H-141/two free fatty acids	PE (18:1/16:0)
Sphingomyelin (SM)		27	15-16	M+H/M+COOH-	M+H	M+H-(18+59)/(M+COOH-)-60	SM (d18:1/24:1)
Glycerolipids (GL)		49	2.0-3.0	M+NH ₄ +	M+NH4+	M+H	TAG (52:6)
Free fatty acid (FFA)		23	2.5-3.5	M-H	M-H	M-H-44	DHA (22:6)
FFA derivatives		65	3.0-6.0	M+NH ₄ +/M-H		N/A	
Sterols		14	2.0-3.0	M+NH ₄ +		N/A	
Others annotated in Lipid MAPS		43				N/A	
Total		403					

N.B. Based on accurate mass searching (\pm 3ppm), the glycerolphospholipids were putatively annotated and classified by using of glycerolphospholipid prediction routine within MZMine 2.10. The other lipids were putatively annotated and classified by interrogating the Lipid Metabolites and Pathways Strategy (Lipid MAPS) database. Reliable MSⁿ fragment data were only obtained on the lipids with sufficient intensity of LC-MS signal at MS level 1, and the example of MSⁿ analysis for each lipid class and subclass is shown in Figure S3.

ESI = electro spray ionisation; TAG = triacylglycerol; DHA = docosahexaenoic acid

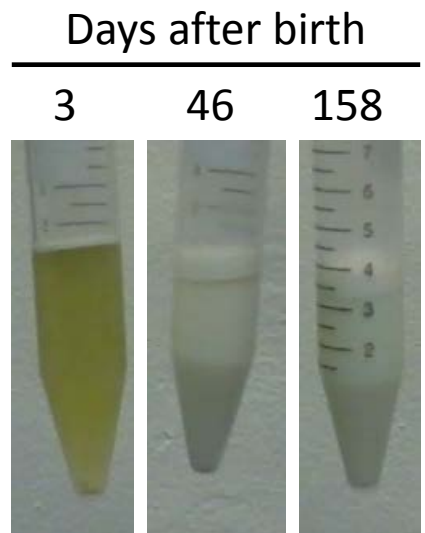


Figure S1 – Changes in appearance of giant panda milk with time, illustrating the changes in colour and fat layer depth. Approximately 4ml samples of milk from giant panda Shu Qing taken on the indicated days post-partum were centrifuged for 15 minutes at 4,500 r.p.m in a bench centrifuge at 4°C.

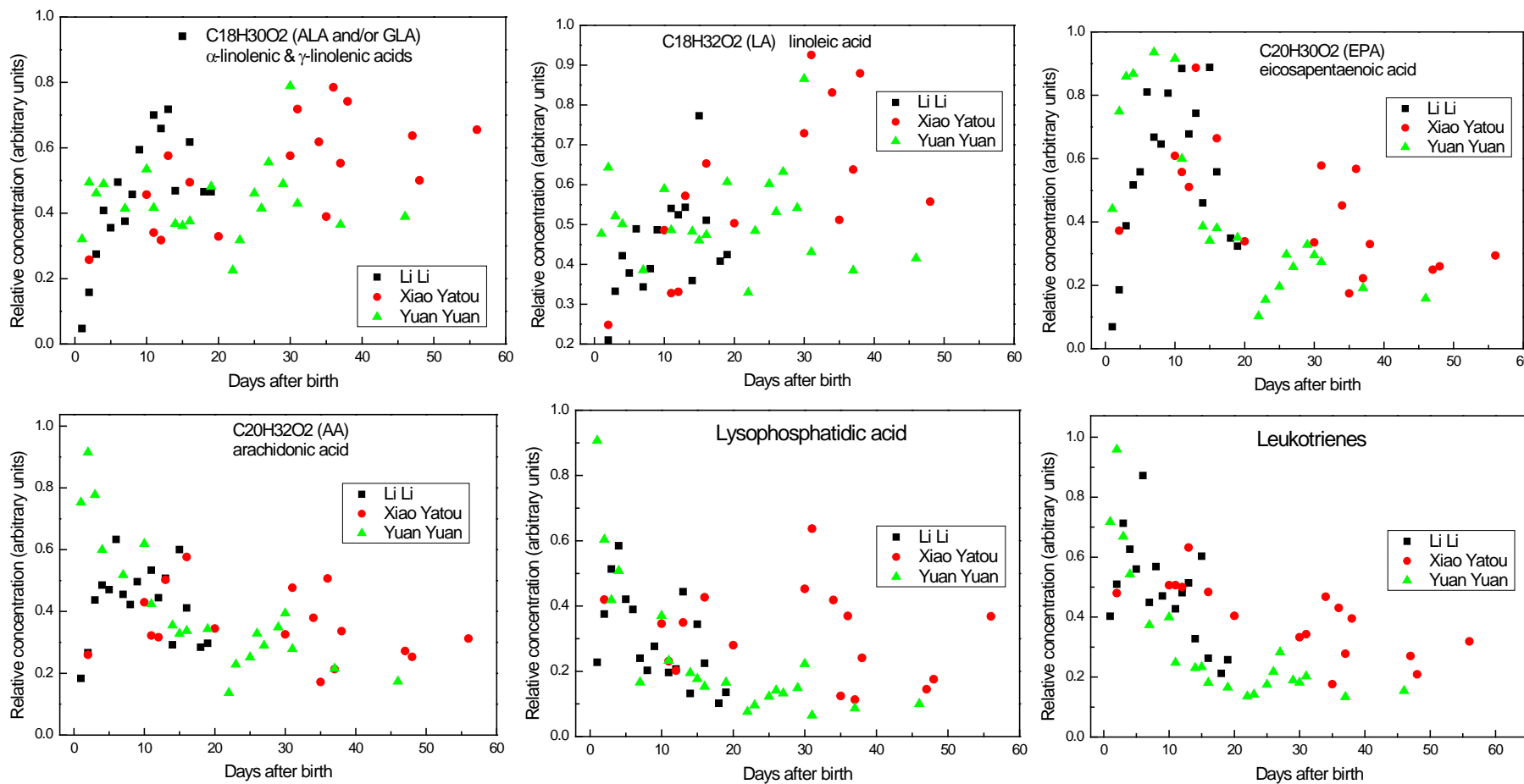


Figure S2. Time courses for selected polyunsaturated fatty acids and lysophosphatidic acid in the milk of three giant pandas with time after birth. ALA and GLA are indistinguishable in the LC-MS analytical system used. Only α-linolenic and linoleic acids are considered to be essential for humans, and are precursors for the others. The leukotrienes plot refers to the non-cysteinyl forms that may include LTA₄ and LTB₄, although also indistinguishable in the LC-MS system used.

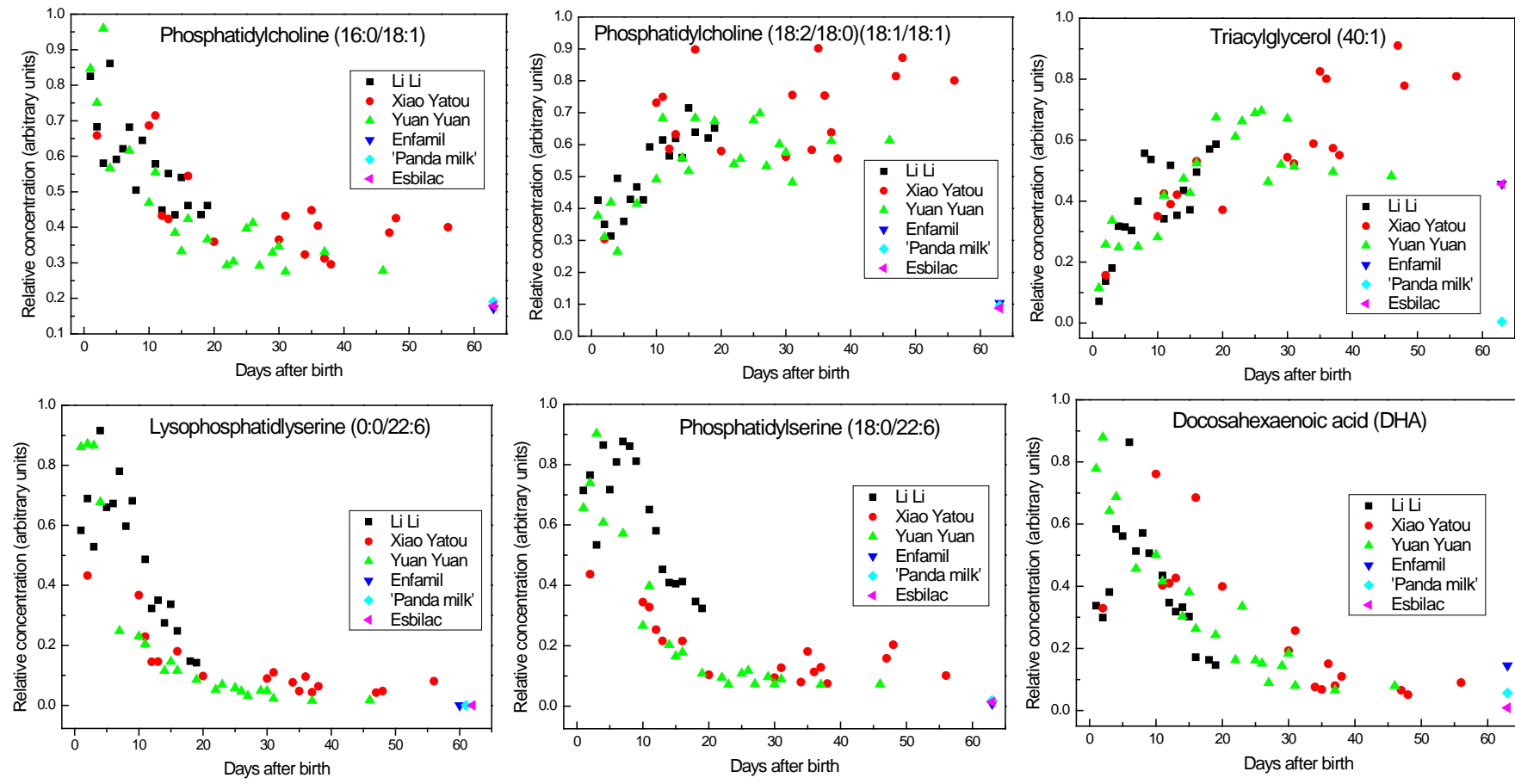
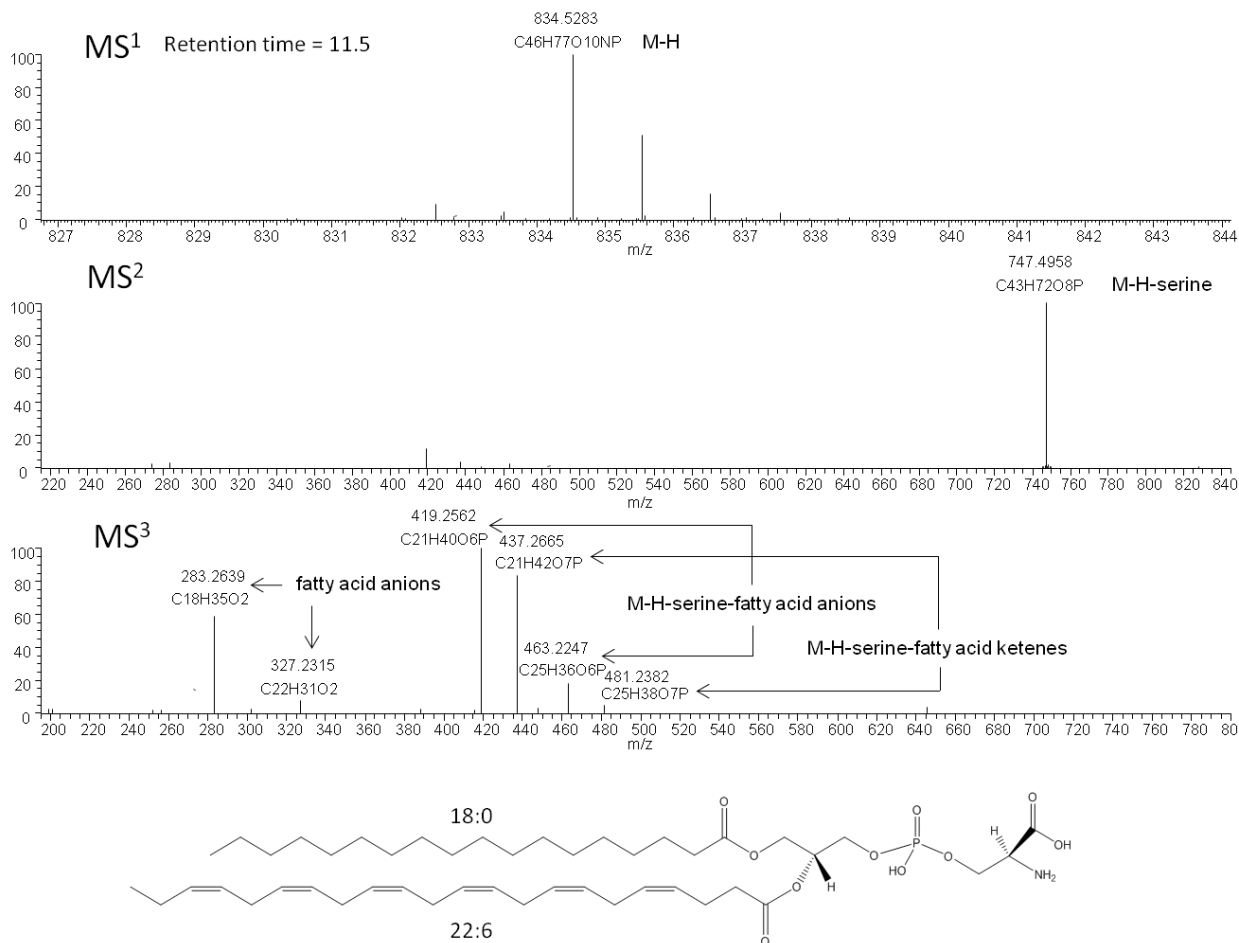


Figure S3. Comparison between the time-dependent lipid profiles of giant panda milk with lipid content of artificial milk replacers. These graphs are the same as in Figure 3 of the main text but here include data for three milk replacers used for giant panda cubs given to the right of each panel. Powdered human infant formula ([®]Enfamil, Mead Johnson, Indiana, USA) and puppy milk replacer ([®]Esbilac, PetAg, Illinois, USA) were obtained from commercial sources. These formulations are currently used directly or as a base for milk substitutes for giant panda cubs. A panda milk replacer (henceforth “Panda milk”), formulated for research use, was obtained from the manufacturer (Morinaga Sunworld Co., Tokyo, Japan) and described in reference [2]. Analysis indicates that this specialist replacer contains little or none of the lipids we find natural to giant panda colostrum (this study), and is also known to contain levels of lactose in excess of those occurring in natural panda milks after day 10 post-partum [1, 3].

Figure S4. Serial mass spectra obtained during identification of lipid species. The first frame is an example of serial mass spectrometry analysis used here for identification phosphatidylserine, followed by MS, MS² and MS³ spectra of the main lipids identified in giant panda milk. Abbreviations - PS, phosphatidylserine; PC, phosphatidylcholine; PI, phosphatidylinositol; PE, phosphatidylethanolamine; SM, sphingomyelin; TAG, triacylglycerol; DHA, docosahexaenoic acid.

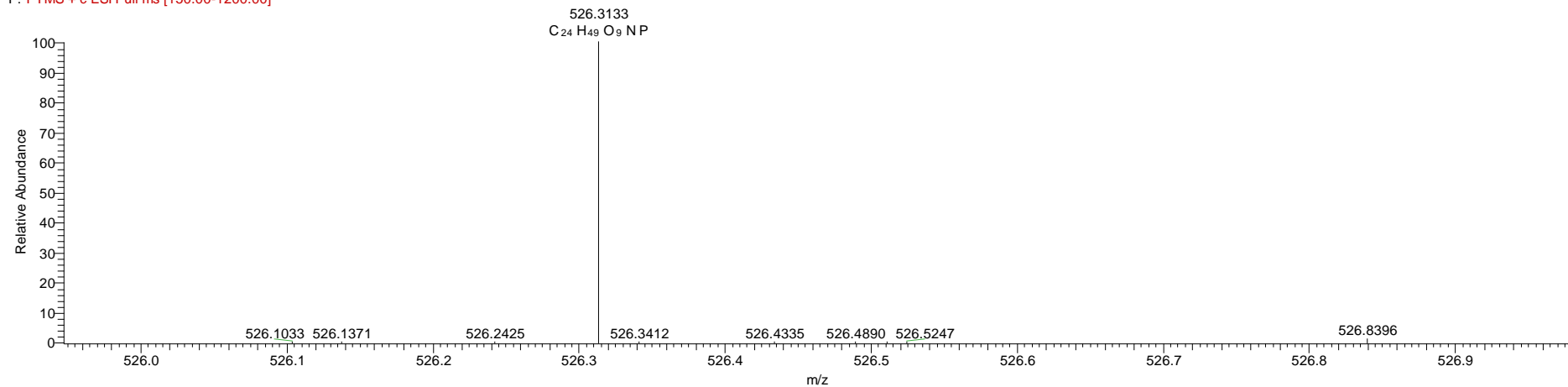


PS (18:0/0:0)

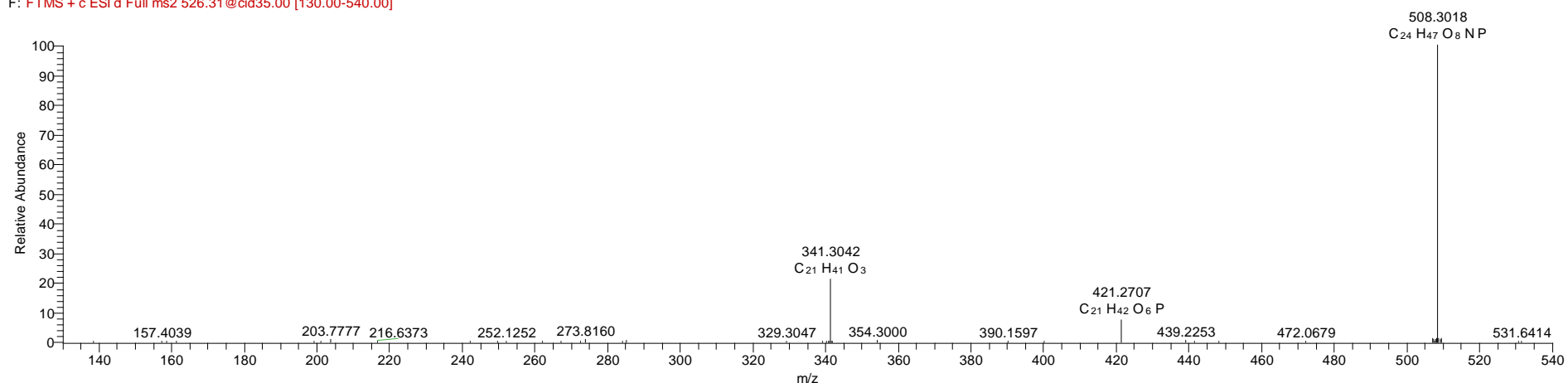
F:\Alex...\Colostrum-Pos-general-2

04/11/2015 21:57:20

Colostrum-Pos-general-2 #472-499 RT: 7.73-8.06 AV: 5 NL: 6.89E5
F: FTMS + c ESI Full ms [150.00-1200.00]



Colostrum-Pos-general-2 #415 RT: 7.84 AV: 1 NL: 7.51E5
F: FTMS + c ESI d Full ms2 526.31@cid35.00 [130.00-540.00]

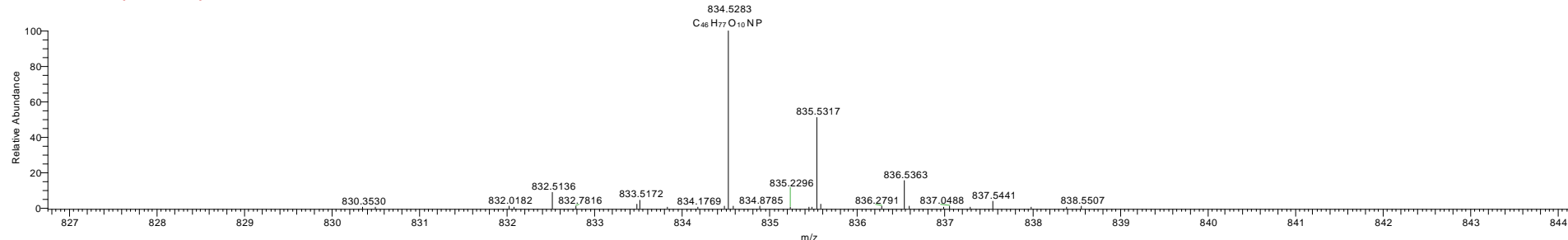


PS (18:0/22:6)

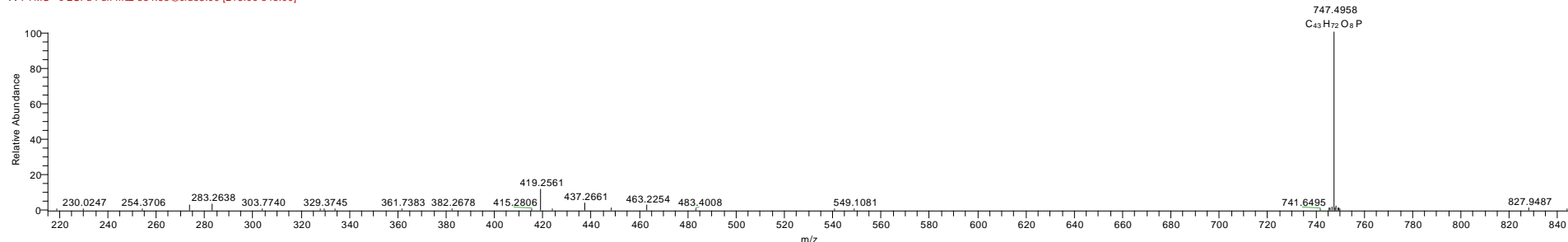
F:\Alex...\Colostrum-Neg-general-2

04/11/2015 18:33:49

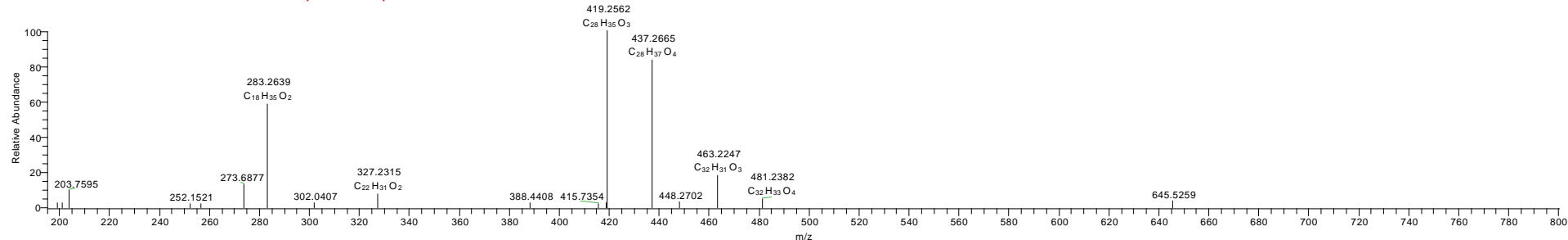
Colostrum-Neg-general-2 #411 RT: 5.67 AV: 1 NL: 2.03E6
F: FTMS - c ESI Full ms [150.00-1200.00]



Colostrum-Neg-general-2 #412 RT: 5.69 AV: 1 NL: 1.03E6
F: FTMS - c ESI d Full ms [834.53@cid35.00 [215.00-845.00]



Colostrum-Neg-general-2 #419 RT: 5.77 AV: 1 NL: 2.09E5
F: FTMS - c ESI d Full ms [834.53@cid35.00 747.50@cid35.00 [195.00-1505.00]

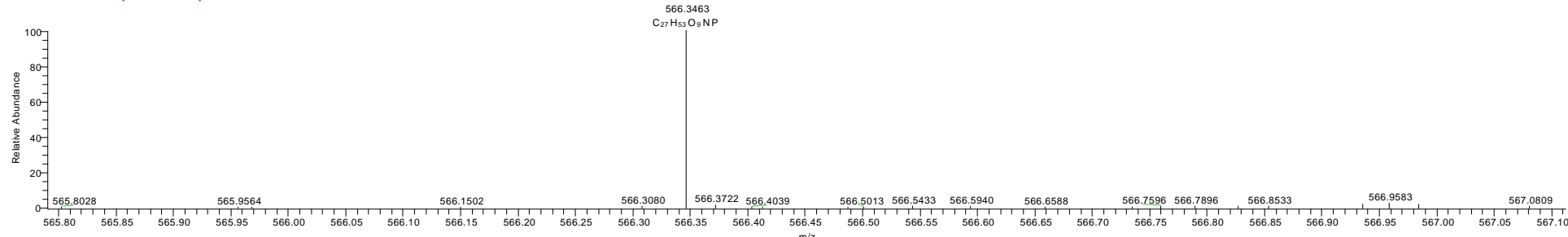


PC (18:1/0:0)

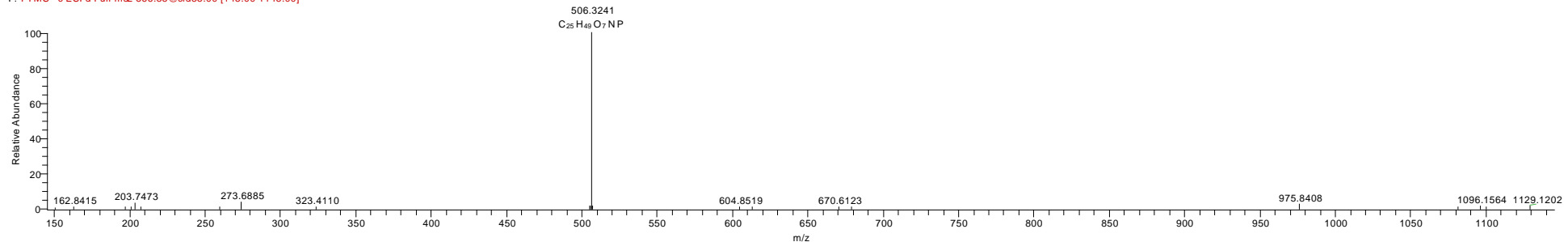
F:\Alex\...\Colostrum-Neg-general-2

04/11/2015 18:33:49

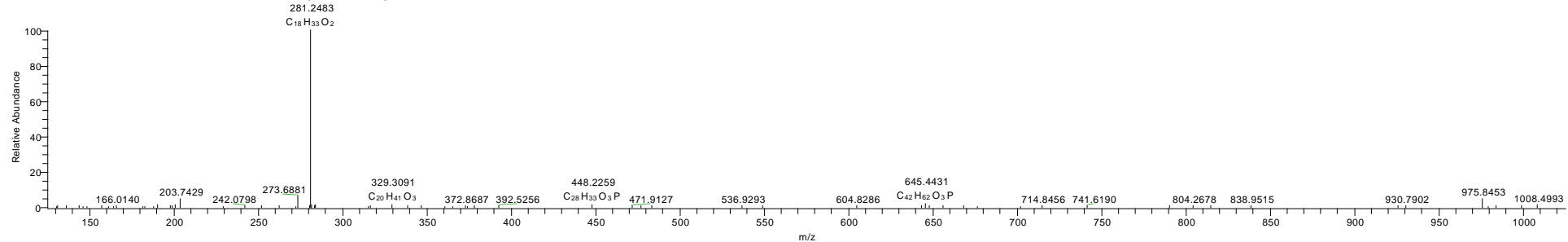
Colostrum-Neg-general-2 #1291 RT: 17.86 AV: 1 NL: 3.68E6
F: FTMS - c ESI Full ms [150.00-1200.00]



Colostrum-Neg-general-2 #1116 RT: 17.51 AV: 1 NL: 6.76E5
F: FTMS - c ESI d Full ms@ 566.35@cid35.00 [145.00-1145.00]



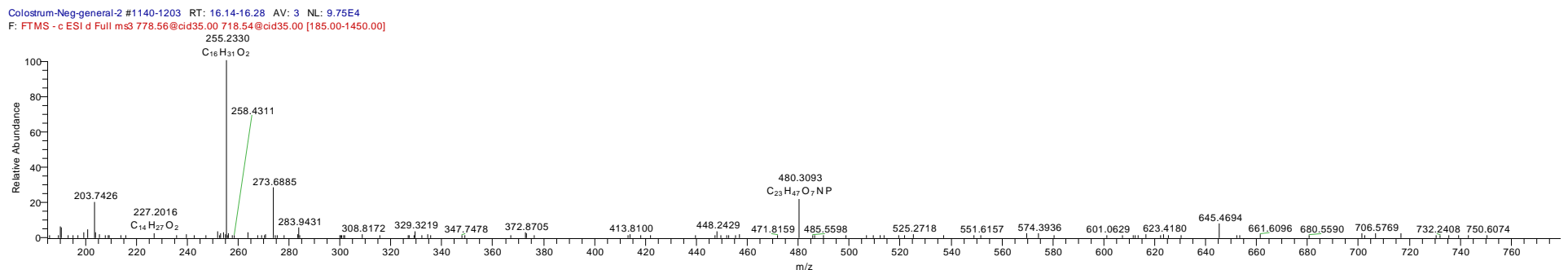
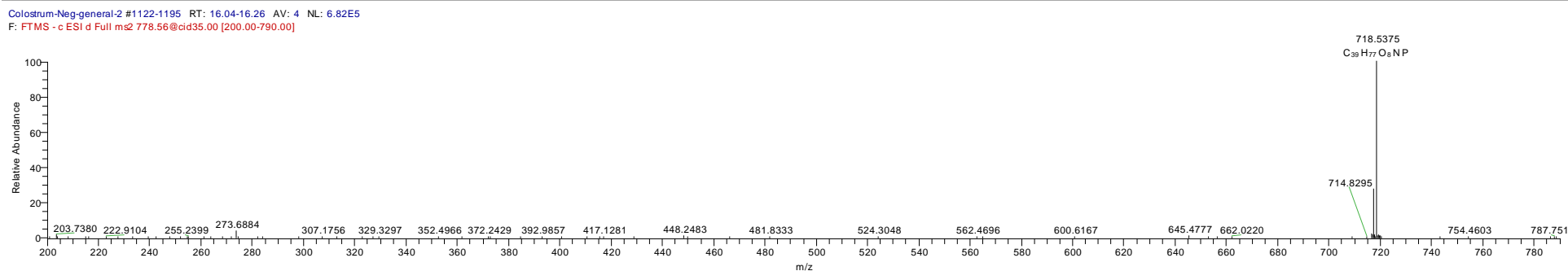
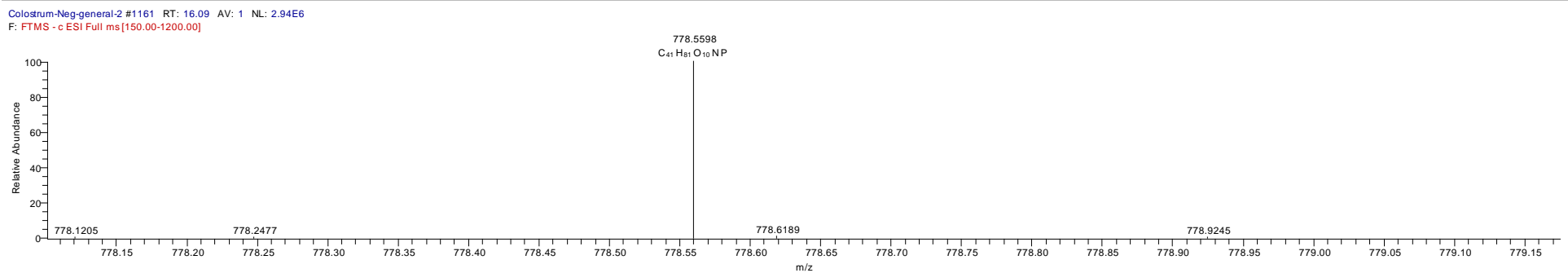
Colostrum-Neg-general-2 #1265 RT: 17.53 AV: 1 NL: 3.93E5
F: FTMS - c ESI d Full ms@ 566.35@cid35.00 506.32@cid35.00 [125.00-1025.00]



PC (16:0/16:0) The PC lipids in negative ion mode are in the form of their formic acid adducts. MS² removes formic acid plus a methyl group, and MS³ gives the fatty acids on the glycerol backbone. In this case, only the negative ion for palmitic acid at m/z 255.2330 can be seen.

F:\Alex...\Colostrum-Neg-general-2

04/11/2015 18:33:49

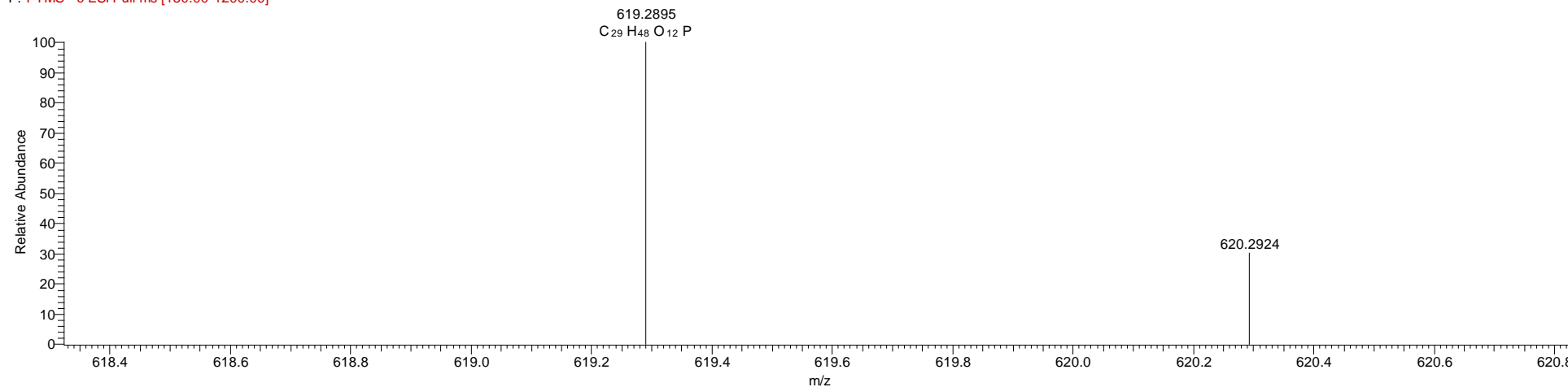


PI (20:4/0:0) In this lyso PI lipid, the negative ion at 303.2327 corresponding to tetracosanoic acid can be seen. The ion at m/z 315.0486 corresponds to the glycerol backbone with phosphoinositol attached following the loss of C20:4.

F:\Alex...\panda milk lipid MS-MS\Neg-2

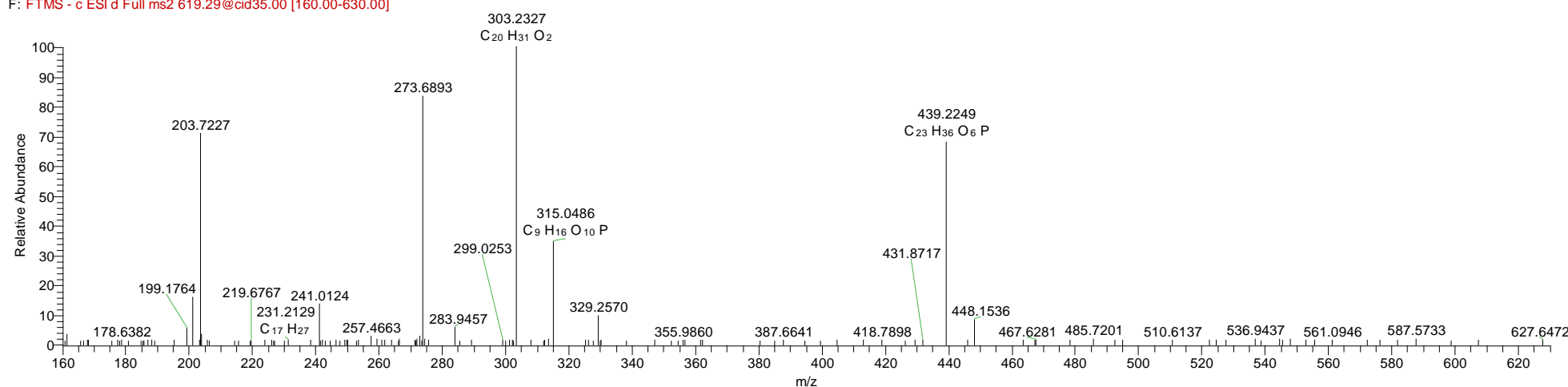
04/11/2015 19:55:11

Neg-2 #271-299 RT: 3.09-3.51 AV: 9 NL: 2.12E5
F: FTMS - c ESI Full ms [150.00-1200.00]



Neg-2 #277-318 RT: 3.19-3.67 AV: 11 NL: 2.92E4

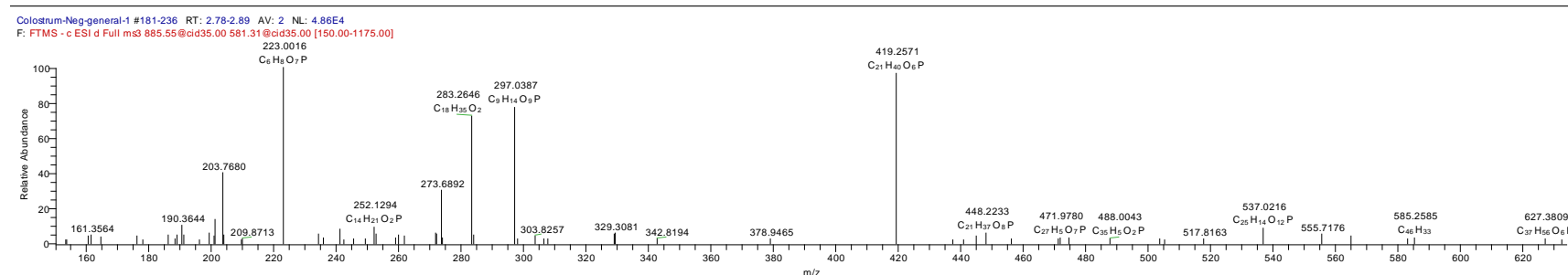
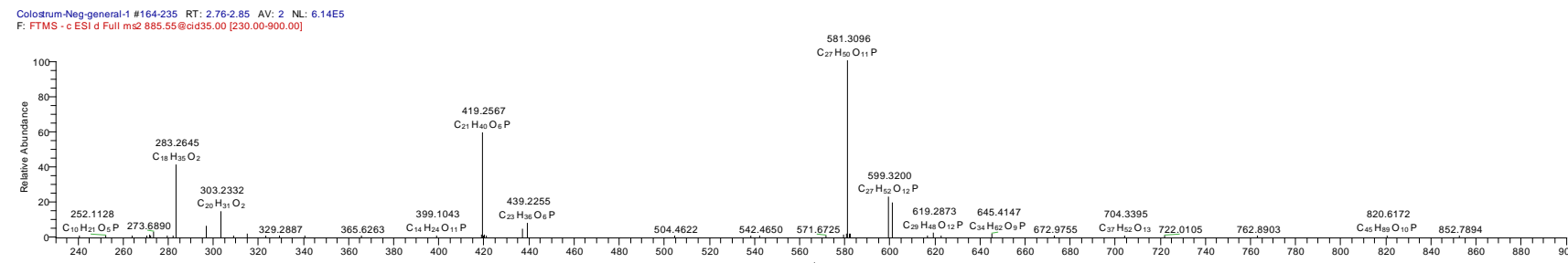
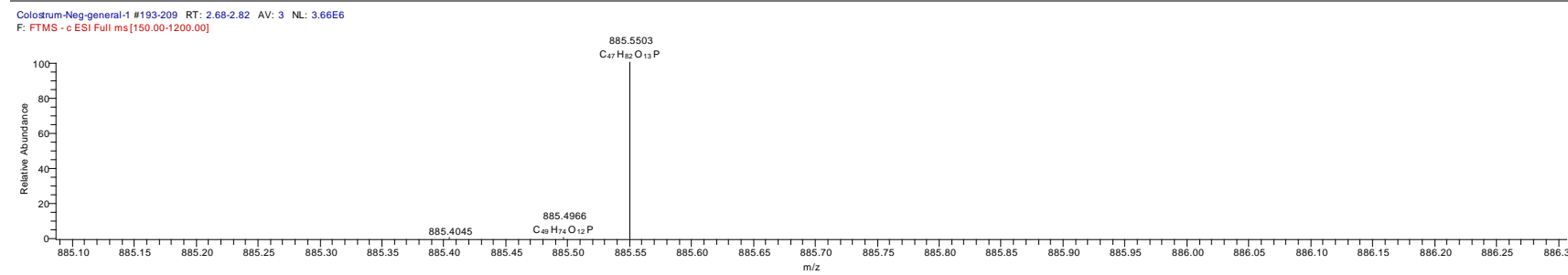
F: FTMS - c ESI d Full ms2 619.29@cid35.00 [160.00-630.00]



PI (20:4/18:0) The MS^2 spectrum shows ions at 283.2645 for C18:0 and at 303.2332 for C20:4. The ion at 588.3096 results from the loss of C20:4 from the molecular ion. There is no evidence of an alternative substitution pattern. MS^3 carried out on 581.3096 produces an ion at 419.2571 due to loss of the inositol. The ion at m/z 297.0387 is due to loss of C18:0 and the ion at 283.2645 is due to the negative ion of C18:0. The ion at m/z 223.0016 is due to inositol phosphate - $2\text{xH}_2\text{O}$.

F:\Alex...\Colostrum-Neg-general-1

04/11/2015 17:53:12

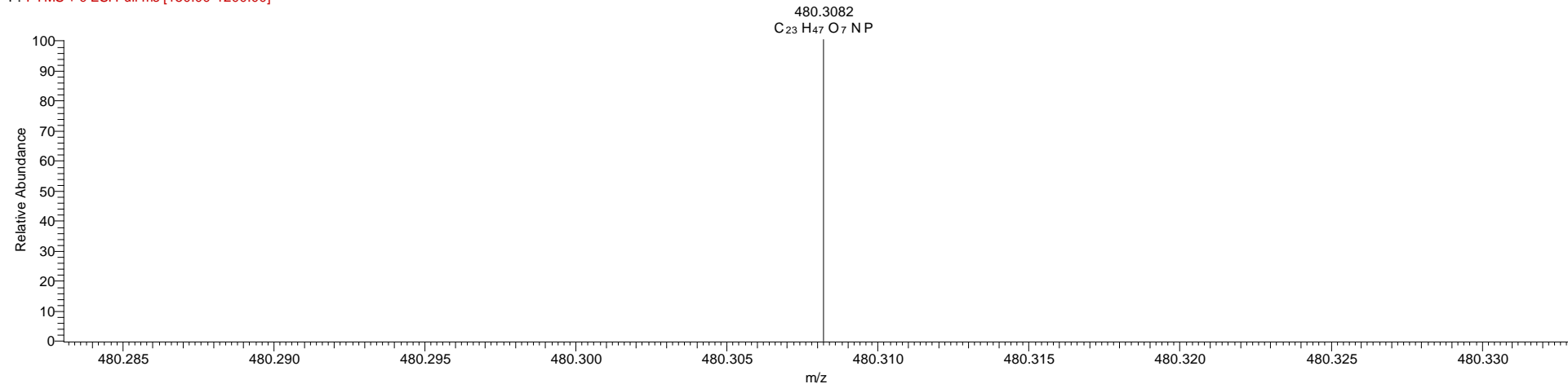


PE (18:1/0:0)

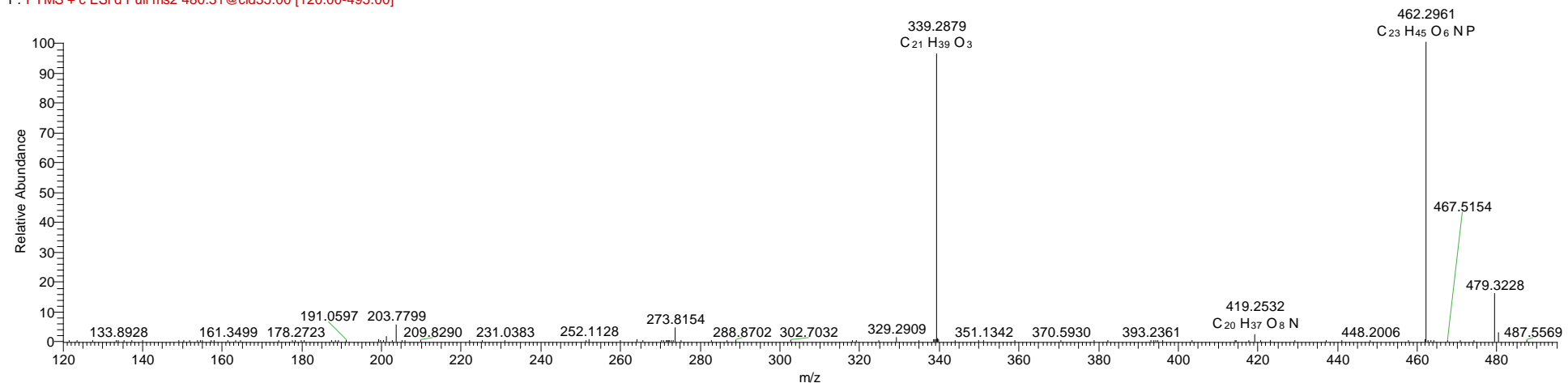
F:\Alex...\Colostrum-Pos-general-3

04/11/2015 22:38:02

Colostrum-Pos-general-3 #534-650 RT: 8.73-10.54 AV: 23 NL: 7.98E5
F: FTMS + c ESI Full ms [150.00-1200.00]



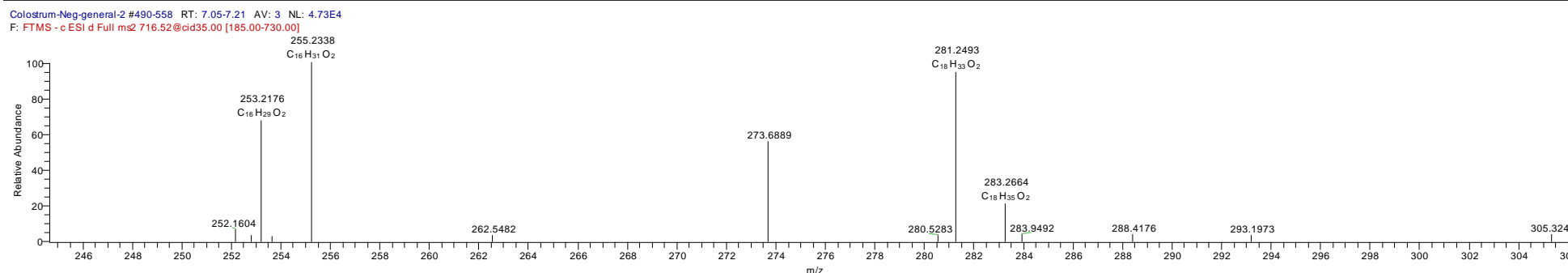
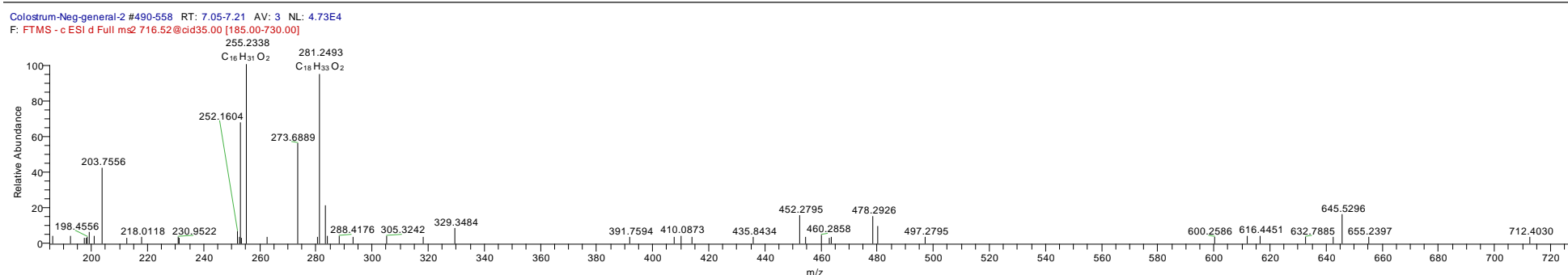
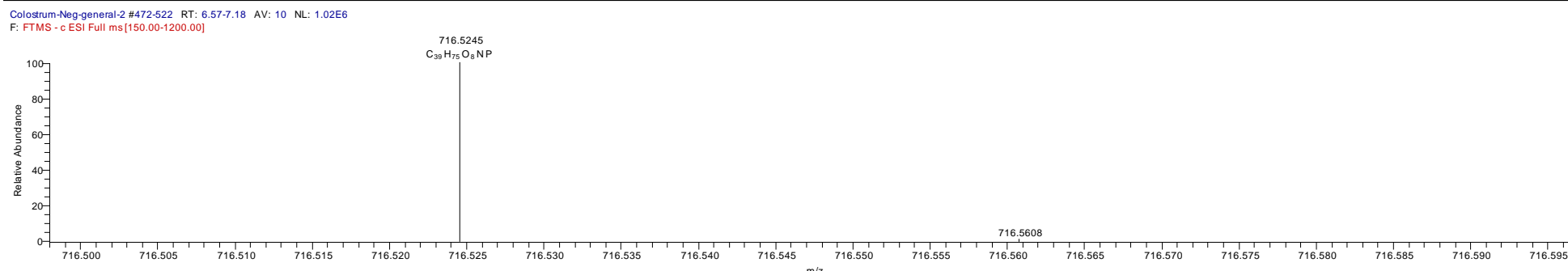
Colostrum-Pos-general-3 #552-627 RT: 9.27-9.92 AV: 7 NL: 9.57E4
F: FTMS + c ESI d Full ms2 480.31@cid35.00 [120.00-495.00]



PE (18:1/16:0)/(18:0/16:1) The ions at m/z 253.2176, 255.2338, 281.2493 and 283.2664 corresponding in C16:1, C16:0, C18:1 and C18:0 indicate that this peak comprises two isomers with different fatty acid chains.

F:\Alex...\Colostrum-Neg-general-2

04/11/2015 18:33:49

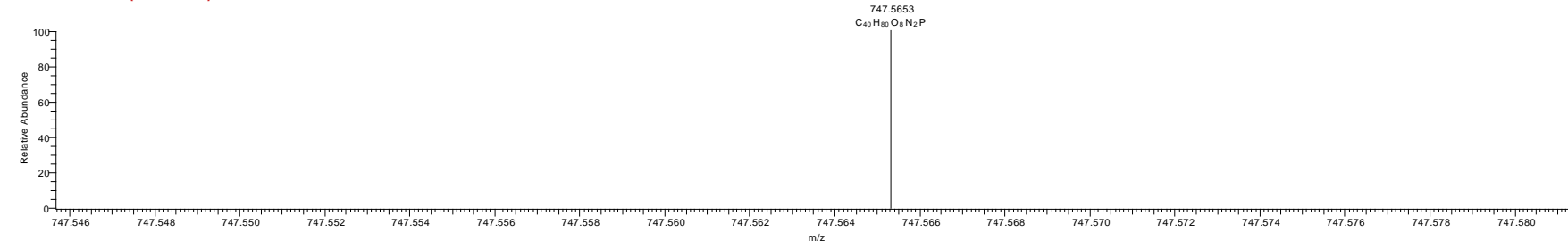


SM (d18:1/16:0) The formula is consistent with a phytosphingolipid which has an additional hydroxyl group in comparison with most mammalian sphingolipids. The additional group may be acetylated since the ion at m/z 687.5437 results from the loss of acetic acid. The MS³ spectrum for the ion at 687.5437 produces a fragment at m/z 616.4716 which must result from the loss of the trimethyl ammonium head group and an extra carbon. The most diagnostic fragment is at m/z 449.3163 which results from the loss of palmitoyl from the amine functionality of the sphingolipid.

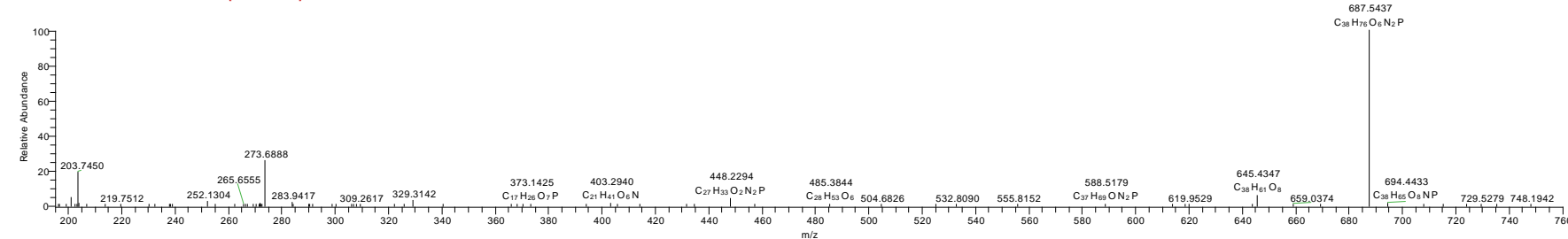
F:\Alex...\Colostrum-Neg-general-2

04/11/2015 18:33:49

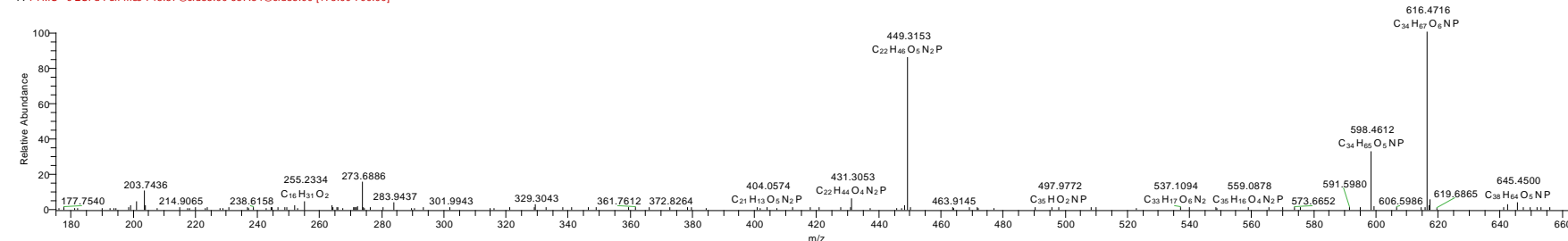
Colostrum-Neg-general-2 #1226 RT: 16.99 AV: 1 NL: 1.34E7
F: FTMS - c ESI Full ms [150.00-1200.00]



Colostrum-Neg-general-2 #1199-1284 RT: 16.93-17.37 AV: 7 NL: 8.77E4
F: FTMS - c ESI d Full ms@747.48 @cid35.00 [195.00-760.00]



Colostrum-Neg-general-2 #1193-1284 RT: 16.97-17.11 AV: 3 NL: 1.29E5
F: FTMS - c ESI d Full ms@748.57 @cid35.00 687.54 @cid35.00 [175.00-700.00]

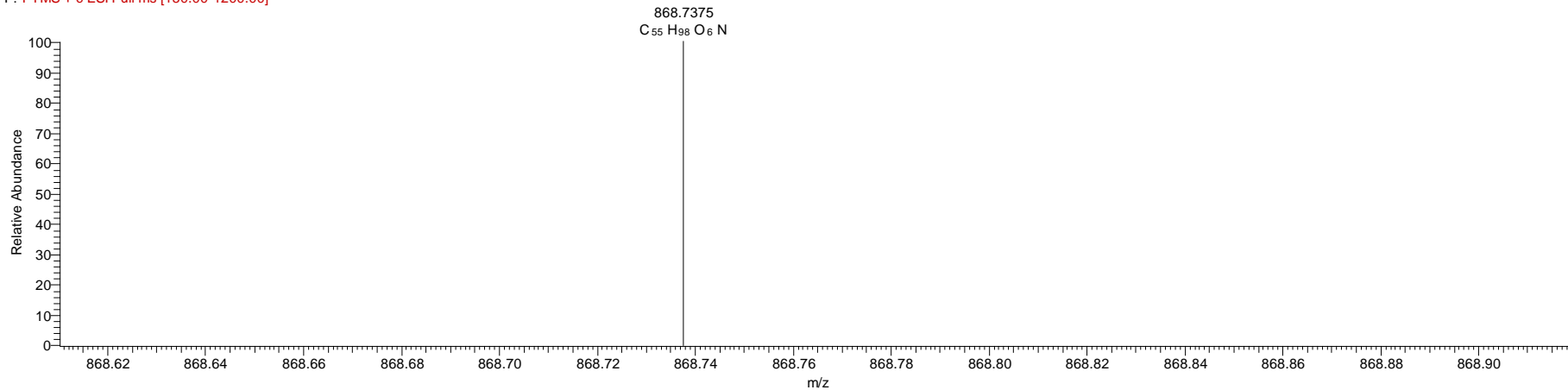


TAG (52:6) Main fatty acids C20:5, C22:6, C16:1, C18:4

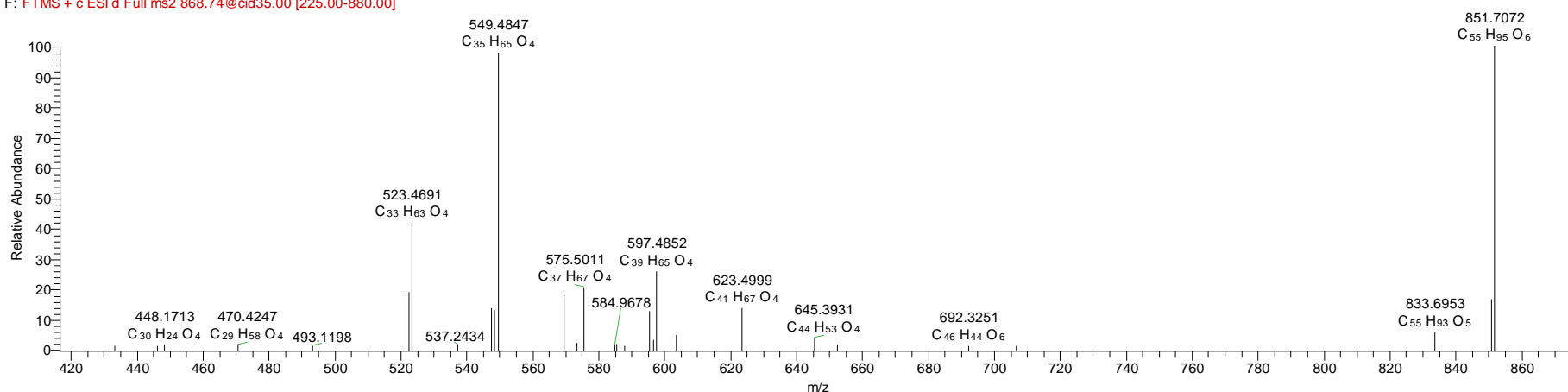
F:\Alex...\Colostrum-Pos-general-2

04/11/2015 21:57:20

Colostrum-Pos-general-2 #133-175 RT: 2.30-2.86 AV: 8 NL: 1.01E6
 F: FTMS + c ESI Full ms [150.00-1200.00]



Colostrum-Pos-general-2 #80-235 RT: 2.49-2.57 AV: 2 NL: 4.70E4
 F: FTMS + c ESI d Full ms2 868.74@cid35.00 [225.00-880.00]

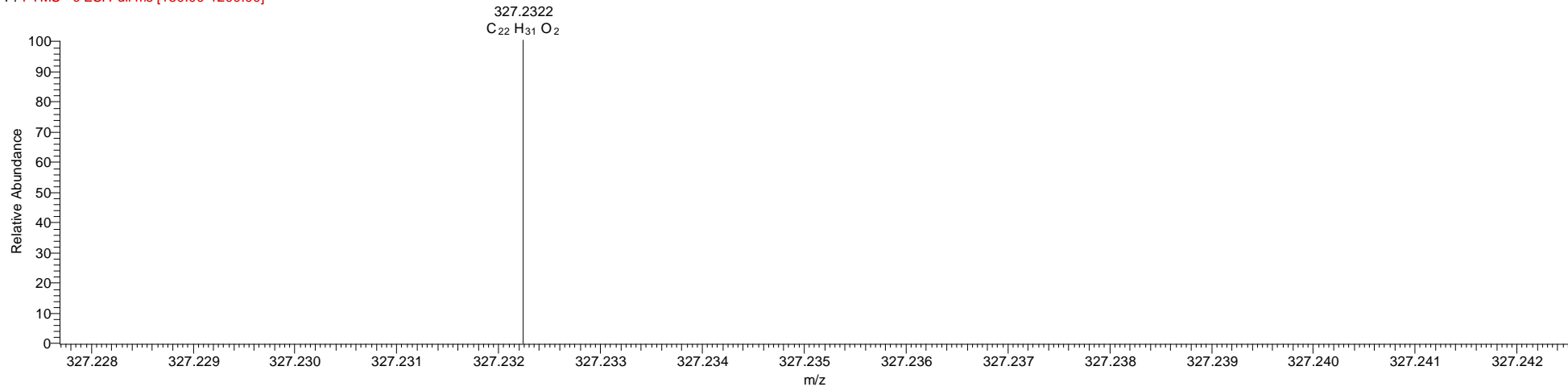


DHA (22:6) The MS² spectrum of DHA shows loss of CO₂ to yield the ion at m/z 283.2430.

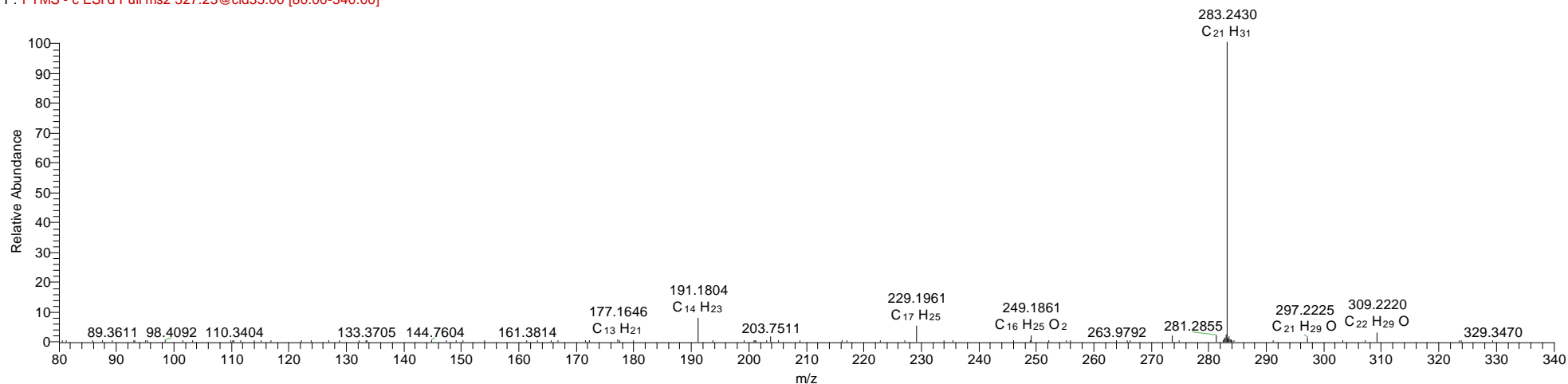
F:\Alex\...\Colostrum-Neg-general-2

04/11/2015 18:33:49

Colostrum-Neg-general-2 #211 RT: 2.90 AV: 1 NL: 4.40E7
F: FTMS - c ESI Full ms [150.00-1200.00]



Colostrum-Neg-general-2 #162-243 RT: 2.80-3.14 AV: 5 NL: 2.93E6
F: FTMS - c ESI d Full ms2 327.23@cid35.00 [80.00-340.00]



References for Supplementary

1. Zhang, T., et al., *Changes in the milk metabolome of the giant panda (*Ailuropoda melanoleuca*) with time after birth - three phases in early lactation and progressive individual differences.* Plos One, 2015. **10**(12): p. e0143417.
2. Zhang, Z., et al., *Analysis of the breast milk of giant pandas (*Ailuropoda melanoleuca*) and the preparation of substitutes.* Journal of Veterinary Medical Science, 2016. **78**(5): p. 747-754.
3. Griffiths, K., et al., *Prolonged transition time between colostrum and mature milk in a bear, the giant panda, *Ailuropoda melanoleuca*.* Royal Society Open Science, 2015. **2**(10): p. 150395.